Supplementary Materials of

The strength of anticipated distractors shapes EEG theta and alpha oscillations in a Working Memory task

Elisa Magosso[1,2*] (0000−0002−4673−2974)

Davide Borra[1] (0000−0003−3791−8555)

[1]Department of Electrical, Electronic and Information Engineering "Guglielmo Marconi" (DEI), University of Bologna, Cesena Campus, Cesena, 47521, Italy

[2]Alma Mater Research Institute for Human-Centered Artificial Intelligence, University of Bologna, Bologna, 40126, Italy

* Corresponding Author

Supplementary Section S1. Event-related spectral perturbations (ERSPs) during memory encoding and retention

In this section we report the event-related spectral perturbations (ERSPs) over time (i.e., obtained during the time course of the working memory task), focusing on encoding and early retention phases, at both scalp and ROI levels. ERSPs were computed as specified in the main text at Section 2.4.3.

1.1. Scalp-level ERSPs

In Figs. S1a, S2a we report the scalp-level theta- and alpha-ERSP mapped onto the scalp over time in the encoding phase and early retention phase. Here, ERSPs were obtained by averaging all epochs together, without separately considering strong and weak distractor conditions, in order to provide a general overview of the time-dependent band-specific spectral changes associated with the encoding and early retention phases of the WM task. Moreover, we provide additional views of the ERSP of representative EEG sensors in Figs. S1b and S2b. Specifically, we report the time-frequency representation of the ERSP of the chosen electrodes in the top panel over the entire frequency range, to provide a comprehensive overview across different EEG bands. Moreover, in the middle panel we report the theta- or alpha-ERSP pattern over time separately for strong and weak distractors, and finally in the bottom panel we report the theta- or alpha-ERSP difference between strong and weak distractor conditions.

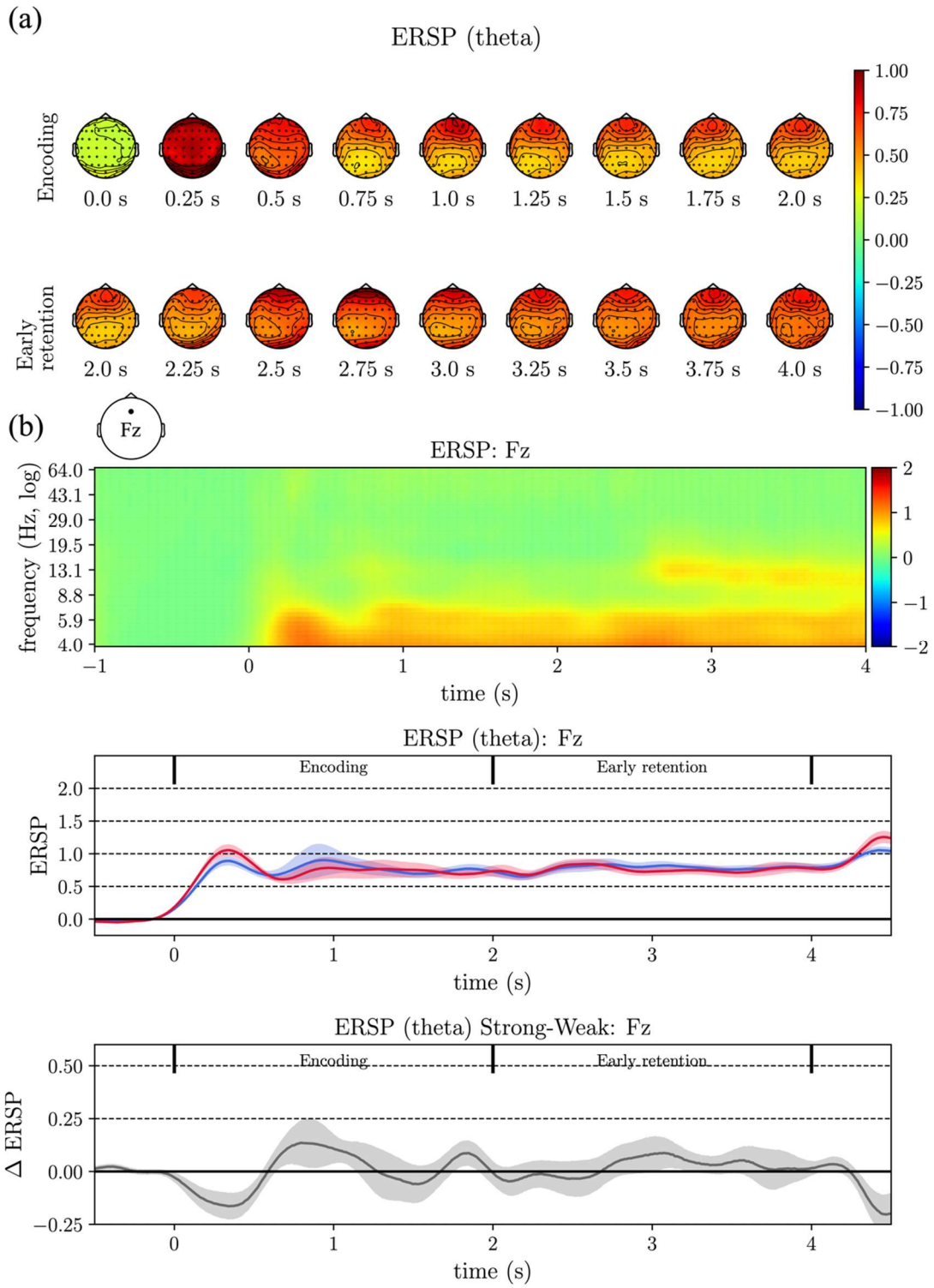

Supplementary Fig. S1 – **Theta-band event-related spectral perturbations at the scalp-level.** *Panel a*: Grand-average theta-ERSP (averaged across distractor conditions) mapped onto the scalp over time during the encoding phase (from 0 s to 2 s) and during the early retention phase (from 2 s to 4 s). *Panel b*: Additional grand-average ERSP representations for one representative electrode site (Fz). Specifically, the time-frequency ERSP is displayed over the entire frequency range in the top panel (mean across distractor conditions), the theta-ERSP temporal dynamics is displayed in the middle panel separately for the strong and weak distractor conditions, and the difference ERSP (Δ_{ERSP}) between the strong and weak distractor conditions is displayed in the bottom panel. In the middle and bottom panels, the mean value (thick line) and standard error of the mean (overlayed area) are reported.

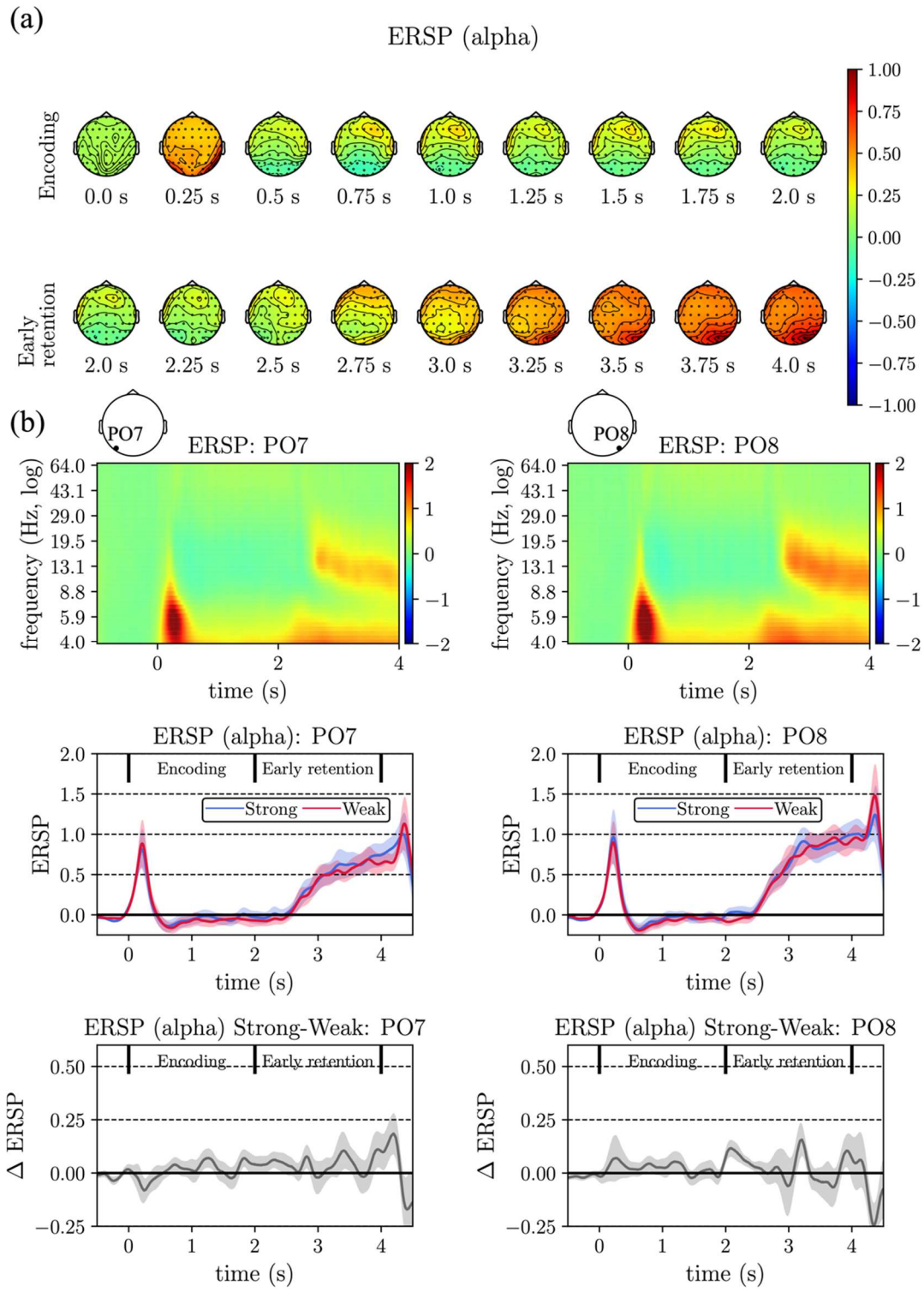

Supplementary Fig. S2 – **Alpha-band event-related spectral perturbations at the scalp-level.** *Panel a*: Grand-average alpha-ERSP (averaged across distractor conditions) mapped onto the scalp over time during the encoding phase (from 0 s to 2 s) and during the early retention phase (from 2 s to 4 s). *Panel b*: Additional grand-average ERSP representations for representative electrode sites (bilateral PO sites, that is, PO7 and PO8). Specifically, for both electrodes, the time-frequency ERSP is displayed over the entire frequency range in the top panels (mean across distractor conditions), the alpha-ERSP temporal dynamics is displayed in the middle panels separately for the strong and weak distractor conditions, and the difference ERSP (Δ_{ERSP}) between the strong and weak distractor conditions is displayed in the bottom panels. In the middle and bottom panels, the mean value (thick line) and standard error of the mean (overlayed area) are reported.

Topological maps of scalp-level ERSPs show that for the theta band (Fig. S1a), a strong frontal and occipital perturbation occurred between 0.25-0.75 s after the onset of the considered phases (encoding and early retention), associated with the evoked response elicited by the changes in the presented visual stimuli, i.e., the presentation of the memory set at 0 s (0.25-0.75 s) and the disappearing of the memory set at 2 s (2.25-2.75 s). In the last 1s-length portion of the encoding phase (encoding TOI), theta-ERSP was mainly focused on frontal electrodes (e.g., around Fz), while in the last 1s-length portion of the early retention phase (retention TOI) theta-ERSP resulted more diffused, assuming largest values also in areas other than the frontal ones (e.g., occipital areas). Since Fz appeared as one of the sites most involved in theta-band perturbations, we focused on this electrode in the additional representations of Fig.S1b. Top panel in Fig. S1b confirms the strong and long-lasting theta-band perturbation at frontal sites. Moreover, frontal theta-ERSP (middle panel of Fig. S1b) was almost constant in the encoding TOI and in the retention TOI for both the strong and weak distractor conditions. Moreover, the bottom panel shows small unsignificant differences between the two distractor conditions in the considered TOIs.

As expected, alpha-ERSP (Fig. S2a) exhibited less evident evoked responses elicited by the changes in the visual stimuli at the onset of each phase (e.g., at 0.25 s), than for theta band. The most relevant alpha perturbations occurred in the retention TOI and were mainly focused on parieto-occipital electrodes, with a clear right-hemisphere bias (centred on PO8). Thus, we focused on this electrode and on its left counterpart (PO7) in the additional representations of Fig. S2b. Top panels of Fig. S2b clearly show a stronger alpha perturbation in the right site (PO8) than left site (PO7). By considering the alpha-ERSP dynamics (middle panels of Fig. S2b), a peculiar progressive increase in the retention TOI was observed, at both hemispheres and in both distractor conditions. Finally, as in case of the theta band, the bottom panels show small unsignificant differences between the two distractor conditions in the considered TOIs.

1.2. ROI-level ERSPs

Here, we enrich the ERSP visualizations by reporting the results also at the cortical ROI-level (Figs. S3 and S4). The results referred to the 28 ROIs (middle column of Table 1 in the main text). We focused on bilateral anterior cingulate ROIs (AC.L and AC.R) as for the theta band, since these regions are considered the main sources of scalp Fz theta activity (Cavanagh and Frank, 2014); we focused on bilateral lateral occipital ROIs (LO.L and LO.R) as to alpha band, since these are the regions approximately underlying the scalp electrodes PO8 and PO7. Similar to the scalp-level analysis, strong theta-ERSP was evident both during encoding and retention, consistently across the two distractor conditions (Fig. S3, top and middle panels). On the other hand, alpha-ERSP was almost null during encoding, and it progressively increased over time during early retention (at the two considered ROIs), consistently across the two distractor conditions (Fig. S4, top and middle panels). Moreover, it is evident the right lateralization in occipital alpha-band ERSP (Fig. S4, middle panels). Finally, the bottom panels show differences across the two distractor conditions larger in the encoding phase for the theta band (Fig. S3 bottom panels) and in the retention phase for the alpha-band (Fig. S4 bottom panels). These differences appeared clearly greater than scalp-level differences (compare with bottom panels in Figs. S1 and S2); indeed, significant differences were found between the two distractor conditions in AC.R theta-ERSP and in LO.L alpha-ERSP (see Fig. 6 in the main text).

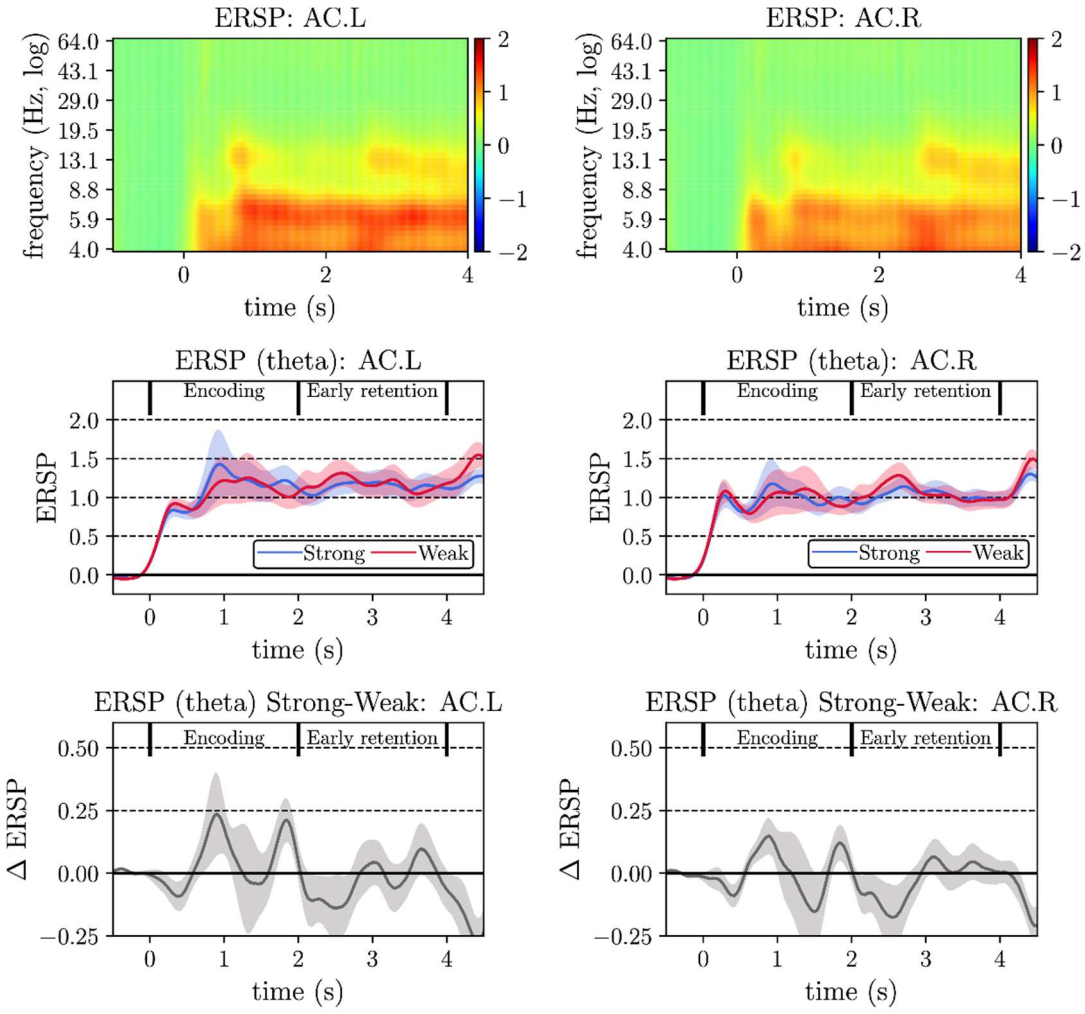

Supplementary Fig. S3 – Theta-band event-related spectral perturbations at the ROI-level. Grand-average ERSP representations for representative ROIs (AC.L and AC.R) are displayed. See the caption of Supplementary Fig. S1b for further details.

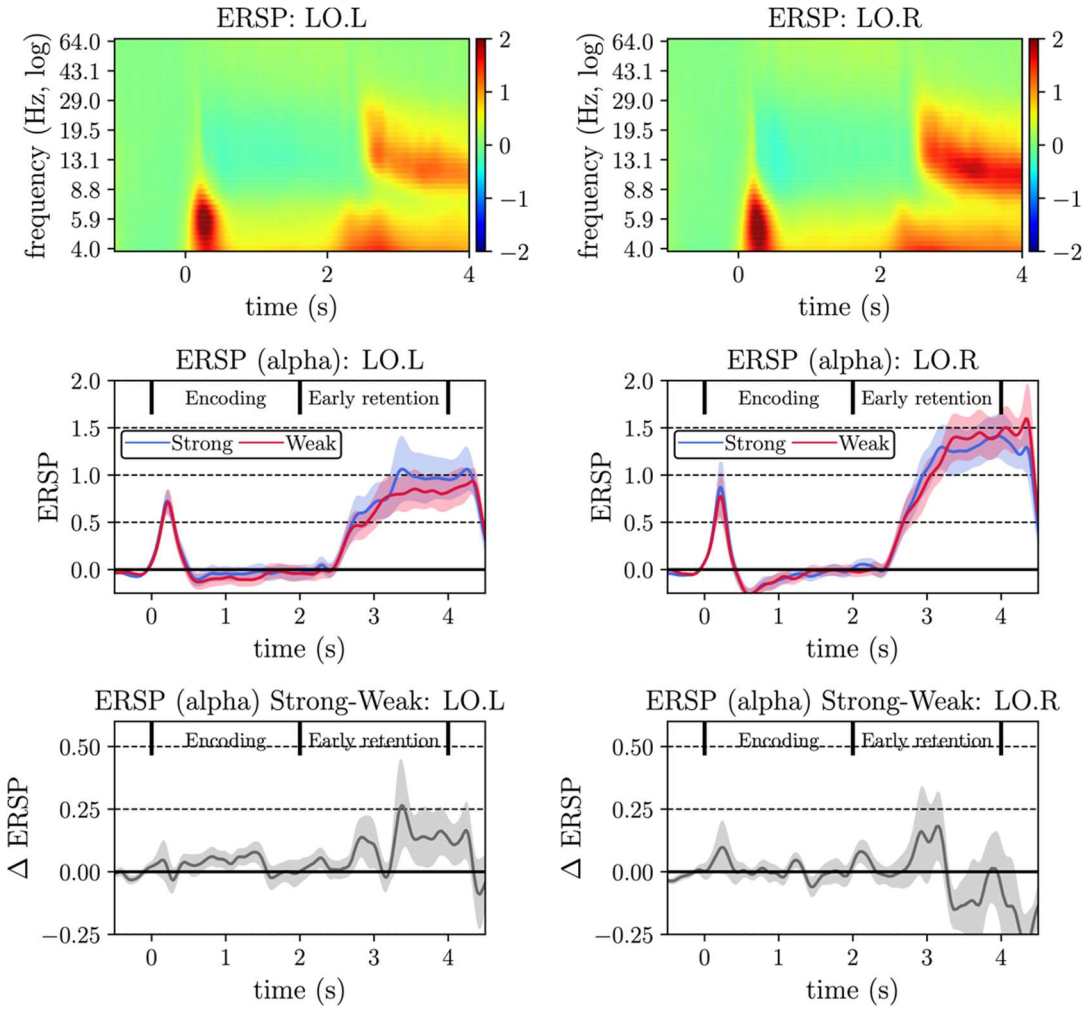

Supplementary Fig. S4 – **Alpha-band event-related spectral perturbations at the ROI-level.** Grand-average ERSP representations for representative ROIs (LO.L and LO.R) are displayed. See the caption of Supplementary Fig. S2b for further details.

Finally, Fig. S5 shows the theta- and alpha-ERSP over time in the encoding TOI and retention TOI, respectively, mapped onto the 28 cortical ROIs. As done for Figs. S1a and S2a, here the ERSPs were obtained by averaging all epochs together, without separately considering strong and weak distractor conditions. These cortical representations reveal a distributed increase of theta power during the encoding TOI, spreading across most of the ROIs, but clearly peaking at frontal and medial-frontal ROIs (including anterior cingulate cortex) and with a right-lateralization (Fig. S5a). Alpha power increased progressively during the retention TOI across widespread areas but peaking in occipital regions and with a right-lateralization evident especially at occipital and temporal regions, assuming the highest values at right-occipital ROIs (Fig. S5b).

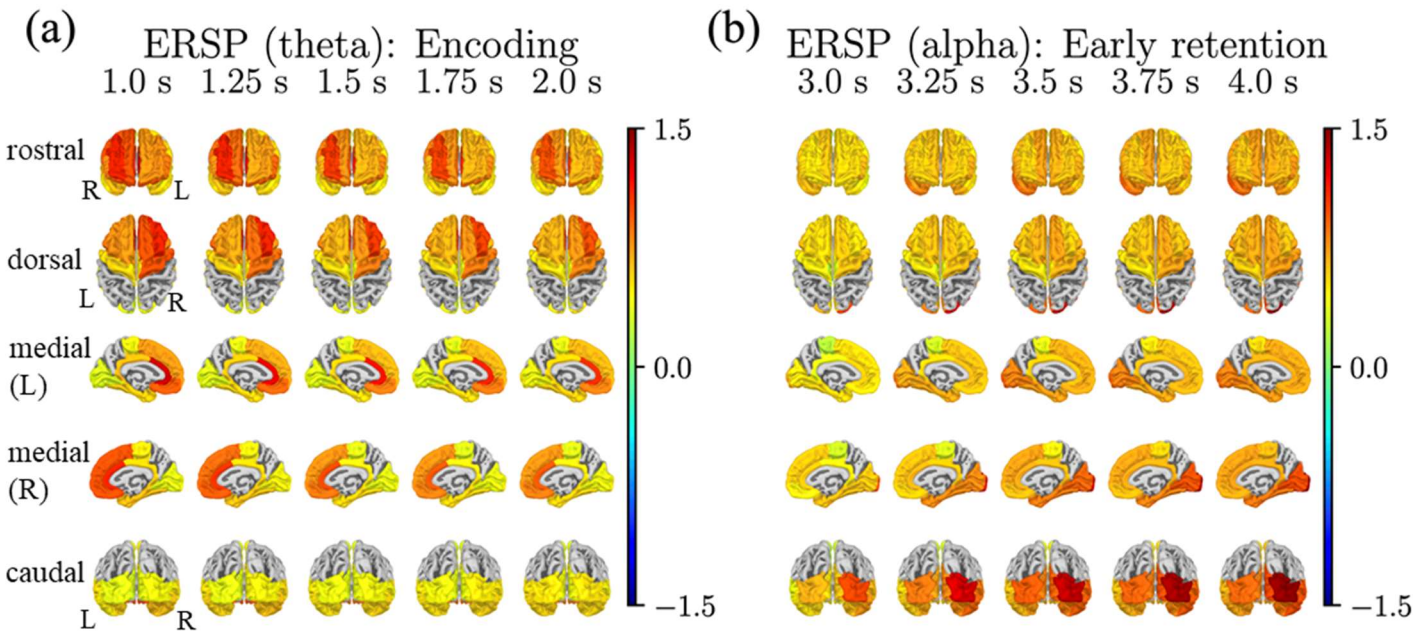

Supplementary Fig. S5 – Theta-band and alpha-band event-related spectral perturbations at the cortex-level within the encoding TOI (theta) and retention TOI (alpha). *Panel a*: Grand-average theta-ERSP (averaged across distractor conditions) mapped onto the cortex during the encoding TOI (from 1s to 2 s). *Panel b*: Grand-average alpha-ERSP (averaged across distractor conditions) mapped onto the cortex during the retention TOI (from 3 s to 4 s). In both panels, cortex views are reported by rows (rostral, dorsal, left-medial, right-medial, caudal, respectively), and time samples within the TOIs by columns. In these figures, parietal cortex is not colored since the analysis was limited to the ROIs covering frontal, occipital and temporal lobes (see main text in Section 2.4.5).

Supplementary Section S2. Connectivity analyses in theta-band during retention and in alpha-band during encoding at lobe-level and at ROI-level

The same procedures described in Sections 2.4.3, 2.4.4 and 2.4.5 of the main text for computing the theta connectivity in the encoding TOI and the alpha connectivity in the retention TOI were replicated here to obtain theta connectivity in the retention TOI (3 s to 4 s) and alpha connectivity in the encoding TOI (1 s to 2 s). We started from the parcel-level connectivity matrices, associated with the alpha band in the encoding phase and theta band in the retention phase, separately for strong and weak conditions. Connectivity values within each of these matrices were aggregated across DK parcels to obtain the connectivity matrices among the 6 macro-ROIs (i.e., lobe connectivity matrices), as detailed in Section 2.4.4 of the main text. The centrality indices (in degree and out degree) associated with the lobe-level connectivity matrices were computed too. Moreover, parcel-level connectivity values were aggregated to obtain the connectivity matrices of the 28 ROIs, obtaining first the complete matrices and then the sparse matrices at the ROI level, and the related centrality indices (in degree and out degree), as specified in Section 2.4.5 of the main text. Moreover, the same statistical analyses described in 2.4.6-ii-iii were performed.

Results are reported in Fig. S6 as to the connectivity analyses at the lobe-level, and in Figs. S7 as to the connectivity analyses at the ROI-level. Note that Fig. S6 (lobe-level analyses) also reports the connectivity and centrality results obtained for the theta band in the encoding TOI and for the alpha band in the retention TOI (already reported and discussed in the main text), for the sake of completeness. Moreover, note that Fig. S7 reports only the results obtained at the ROI-level for the theta band in the retention TOI and not for the alpha band in the encoding TOI; indeed, no ROI exhibited significantly different in degree or out degree in case of strong vs. weak distractors in the alpha band during the encoding TOI.

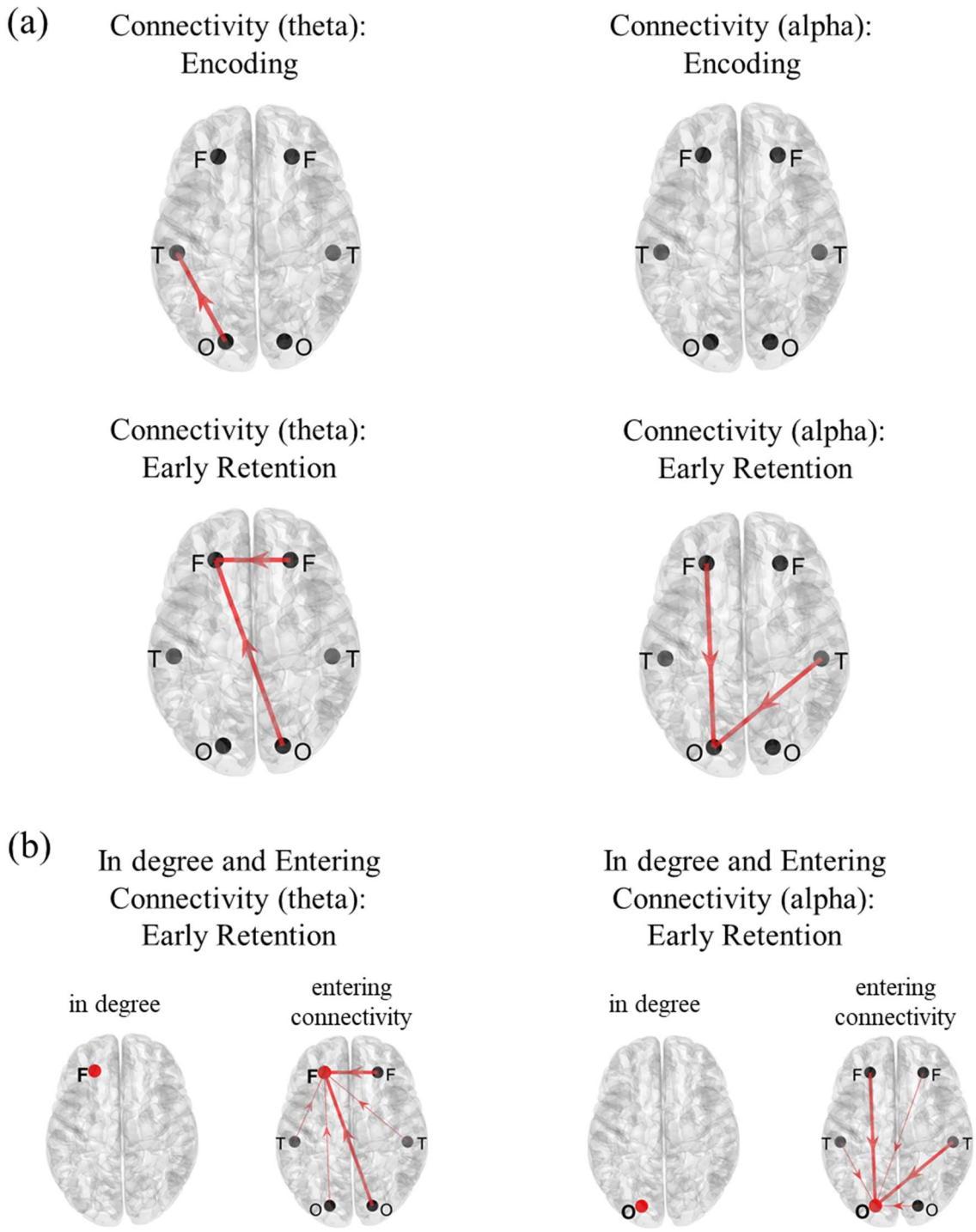

Supplementary Fig. S6 – Lobe-level connectivity analysis in both encoding and early retention: comparison between strong and weak distractor conditions. Here, theta-band results are displayed in the left panels, while alpha-band results are displayed in the right panels. *Panel a*: Each node represents a lobe (F: frontal, T: temporal, O: occipital) and the displayed directed edges indicate connections significantly higher for strong compared to weak distractors ($p<0.05$, uncorrected). *Panel b – top panels*: Lobes with significantly higher in degree index in the strong vs. weak distractor condition ($p<0.05$, uncorrected) and connections entering into these lobes, higher for strong vs. weak distractors (thicker lines denote significant connections, $p<0.05$, uncorrected). As already reported in the main text, no lobe exhibited higher in degree or out degree for strong vs. weak distractors in the theta band during encoding and no lobe exhibited higher out degree for strong vs. weak distractors in the alpha band during retention. Moreover, in the alpha band during encoding, no lobe exhibited higher in degree or out degree for strong vs. weak distractors.

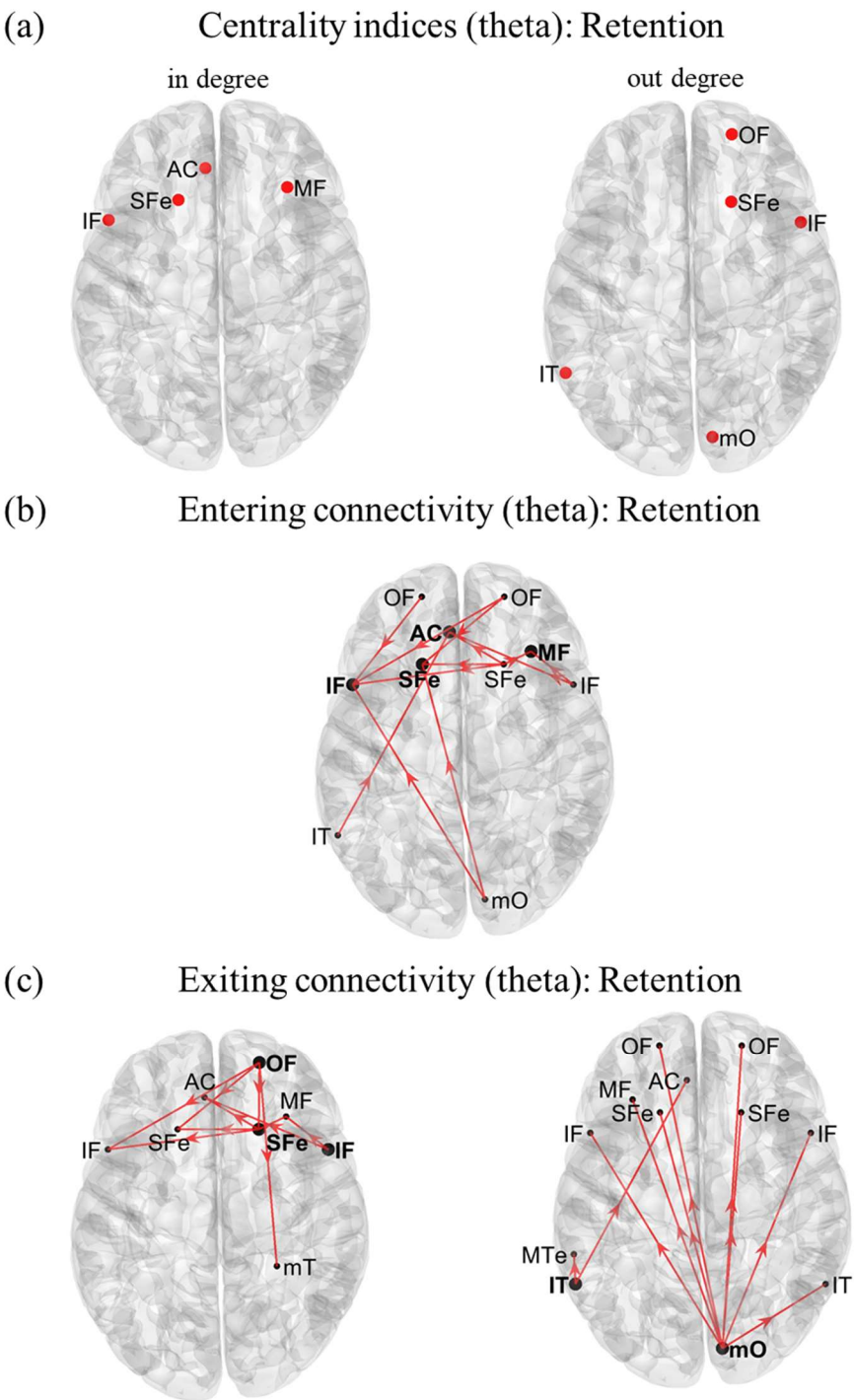

Supplementary Fig. S7 – ROI-level connectivity results: comparison of theta-band connectivity during early retention between strong and weak distractor conditions. *Panel a*: ROIs with a significantly higher ($p < 0.05$, corrected) in degree (left panel) and out degree (right panel) in the strong vs. weak condition, when considering theta-band connectivity in the retention TOI. *Panel b*: Connections entering in a selection of ROIs with significant in degrees (from panel a). Red/blue arrows denote an increased/decreased connectivity in strong vs. weak condition; only significant connections ($p < 0.05$) are displayed. *Panel c*: Connections departing from a selection of ROIs with significant out degrees (from panel a). Red/blue arrows denote an increased/decreased connectivity in strong vs. weak condition; only significant connections ($p < 0.05$) are displayed.

No figure is reported for the alpha-band connectivity at the ROI-level during the encoding TOI, since no ROI exhibited significantly different in degree or out degree in case of strong vs. weak distractors in the alpha band during the encoding TOI.